AIAA JOURNAL
Vol. 31, No. 12, December 1993

Investigation of the Stress Distributions in Corner Tensioned Rectangular Membranes

D. J. Gorman*
University of Ottawa, Ottawa, Ontario K1N 6N5, Canada
R. K. Singhal† and W. B. Graham‡
Canadian Space Agency, Ottawa, Ontario K2H 8S2, Canada
and
J. M. Crawford§
Dynacon Enterprises, Ltd., Downsview, Ontario M3H 5T5, Canada

A study is made of the stress distributions induced in rectangular membranes by concentrated outward corner loads acting along the diagonals. Two methods of analysis are employed. An analytical study is conducted by means of superimposed Airy stress functions. This study is complemented by a parallel study conducted with a commercially available finite element program. Very good agreement is obtained when results of the two studies are compared.

Nomenclature

a, b = membrane edge lengths
x, y = distances along coordinate axes
δ = distance from concentrated applied force to corner of membrane
ξ = x/a
σ_x, σ_y = normal stresses
τ_{xy} = shear stress

Introduction

THE Department of National Defence (DND) has been pursuing a technology development program relative to the space-based radar (SBR)[1] system for a number of years. A key area of technology is structural dynamics. Several of the satellites proposed, as well as some of their subsystems, are classified as large space structures (LSS). Typically, LSS are lightweight, structurally very flexible, have low natural frequencies of vibration, exhibit low damping, and are connected by or possess nonlinear joints. The need to develop methods of synthesizing test results and/or analytical and test results as well as methods of testing large subsystems to predict on-orbit performance is recognized in the space community.

The tensioned membrane is a structure that has already had significant use in space systems. It is of special interest to SBR, since one of the proposed SBR systems involves a membrane-type radar array, referred to as the space-fed system, of approximately football-field size which perhaps represents the ultimate in lightweight structures. It is of interest as well to many large space systems, including other SBR proposed satellite designs, because solar arrays may be constructed similarly.

The subject of this paper represents a single step toward a more general goal with respect to the development of structural dynamics analytical and testing techniques for tensioned membranes which involves the investigation in methods of continuum mechanics, finite element methods (FEM), and modal testing methods. Three objectives motivate the present work which focuses on a thin rectangular membrane subjected to equal, concentrated forces acting outwardly at the corners of the membrane in directions coincident with the diagonals of the membrane, and these are 1) to obtain a continuum mechanical solution for the stress distribution; 2) to obtain a FEM solution for the stress distribution; and 3) to compare the results of both analyses.

The stress analysis is essential to ensure that wrinkling of the membrane, a completely unacceptable phenomenon, will be avoided. The wrinkling phenomenon will be discussed in detail later. Also, the stress analysis is a point of verification along the way toward the prediction of modal frequencies and shapes (and subsequent comparison with modal test results). This paper provides a brief description of the analysis techniques and presents a comparison of the computed data.

Computation of Stress Distributions

Continuum Mechanical Approach

The continuum mechanical approach is based on the Airy stress function. Because the details of the technique employed will appear in a forthcoming publication,[2] only a brief description will be

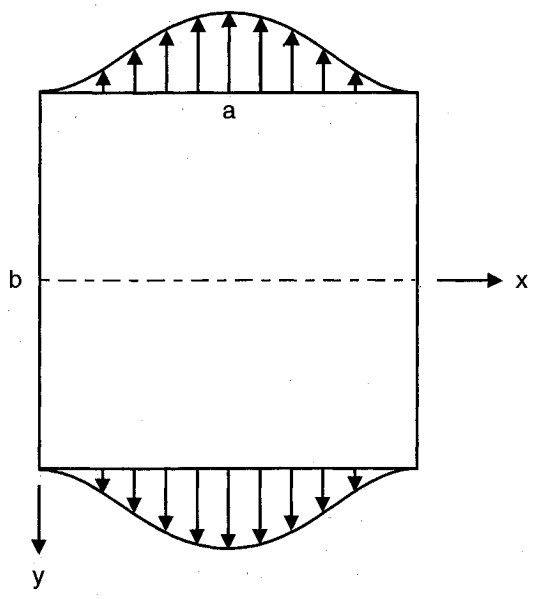

Fig. 1 Rectangular membrane loaded with outward-acting symmetrically distributed loading on two opposite edges.

Received Dec. 14, 1992; revision received May 10, 1993; accepted for publication May 11, 1993.

*Professor, Department of Mechanical Engineering.
†Senior Structural Dynamicist, P.O. Box 11490 Station H.
‡Manager, Dynamics Research, P.O. Box 11490 Station H.
§Junior Research Engineer, 5050 Dufferin St., Suite 222.

provided here. It is essentially an extension of the technique described by Timoshenko and Goodier.[3] Three judiciously selected Airy stress function solutions are expressed in the form proposed by Lévy as found in Ref. 4. The stress functions are then superimposed, and following procedures identical to those employed in the free vibration analysis of plates[5] the Fourier coefficients appearing in the combined solutions are constrained so as to satisfy the prescribed boundary conditions.

Consider a membrane problem, referred to hereafter as a building block, as shown in Fig. 1. The rectangular membrane has equal outward acting edge loading distributed along the edges $y = \pm b/2$. Furthermore, these same edges are free of shear forces. The edge loading is symmetric also with respect to the central axis $x = a/2$. The stress function for this problem can be written as

$$\phi(x, y) = \sum_{m=1,3}^{\infty} Y_m(y) \sin\frac{m\pi x}{a} \tag{1}$$

Substituting this function into the compatibility equation, and taking advantage of the symmetry about the x axis, we obtain[3]

$$Y_m(y) = C_{1m}\cosh\ \alpha y + C_{2m}\, y\, \sinh(\alpha y) \tag{2}$$

where $\alpha = m\pi/a$.

We choose to represent the applied edge normal stress of the building block of Fig. 1 as

$$\sigma_y(x) = \sum_{m=1,3}^{\infty} A_m \sin\frac{m\pi x}{a} \tag{3}$$

We recall the relationship between the stress function and the in-plane stresses, i.e.,

$$\sigma_x = \frac{\partial^2\phi(x,y)}{\partial y^2}, \qquad \sigma_y = \frac{\partial^2\phi(x,y)}{\partial x^2}, \qquad \tau_{xy} = \frac{\partial^2\phi(x,y)}{\partial x \partial y} \tag{4}$$

Enforcing the zero shear stress condition along the loaded edges of the building block, as well as the condition expressed by Eq. (3), we can readily evaluate the constants C_{1m} and C_{2m} of Eq. (2). With these constants evaluated we now have available the stress function for the first building block in our solution. It is readily shown that although this building block is free of normal stress σ_x along the edges $x = 0$ and $x = a$, there exists a nonzero shear distribution along these same edges. Let us suppose we wish to eliminate this shear stress without adding shear stress to the edges $y = \pm b/2$. We also wish to end up with a combined final solution where the only edge normal stresses are those given by Eq. (3).

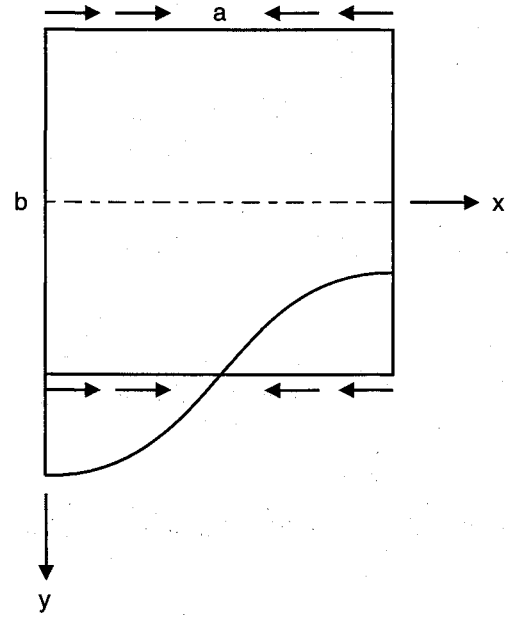

Fig. 2 Rectangular membrane building block subjected to shear stress distribution along opposite edges.

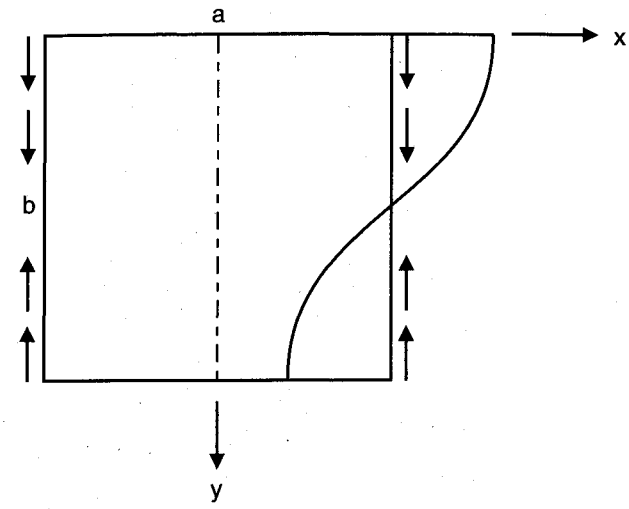

Fig. 3 Rectangular membrane building block subjected to shear stress distribution along opposite edges.

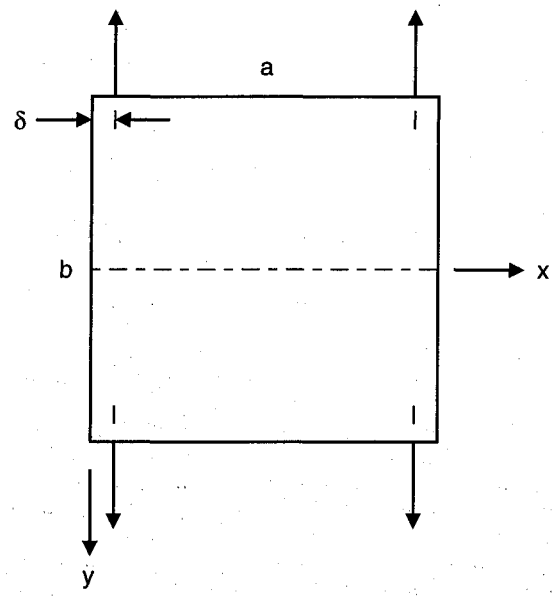

Fig. 4 Rectangular membrane subjected to equal concentrated forces along opposite edges at distance δ from corners.

We achieve this end by adding two more building blocks to the first. Consider next the building block represented schematically in Fig. 2. Here the edges $y = \pm b/2$ are free of normal stress but are subjected to a shear stress antisymmetric with respect to the central axis $x = a/2$ and whose distribution is represented as

$$\tau_{xy} = \sum_{m=1,3}^{\infty} A'_m \cos\frac{m\pi x}{a} \tag{5}$$

The solution for this second building block is taken in a form identical to that of the first building block [Eq. (1)]. Following identical steps and enforcing the prescribed edge conditions we obtain its solution in similar form, as given by Eq. (2). Of course, the expressions for the constants C_{1m} and C_{2m} will be different.

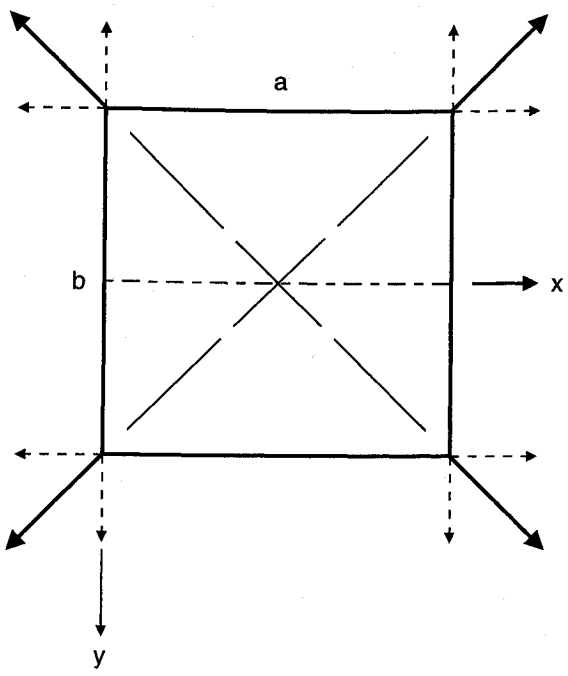

Fig. 5 Rectangular membrane subjected to equal concentrated tensile loads at each corner.

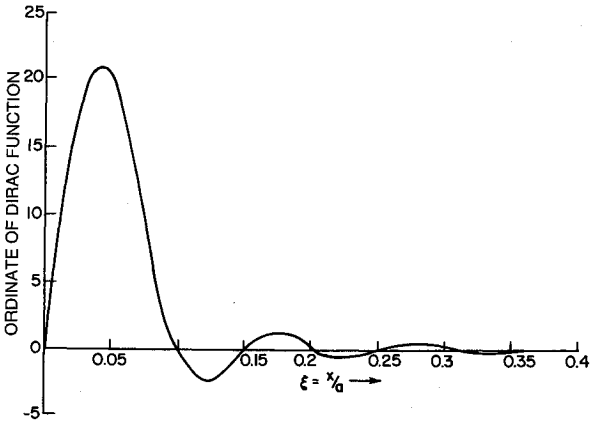

Fig. 6 Plot of truncated series representation of Dirac function k = 10, $\delta/a = 0.05$: vertical line at $\xi = 0.05$ indicates desired center of load to be represented by this function.

Note that again the edges $x = 0$ and $x = a$ will have shear stress distributed along them but all edges will be free of normal edge reaction.

Finally, we generate the solution for the building block of Fig. 3. This problem differs from that of Fig. 2 in that the edges $x = \pm a/2$ are prescribed free of normal stress, with imposed shear stress prescribed in the form of Eq. (5), the coordinates x/a replacing y/b. In fact, the solution for this third building block is obtained by simply interchanging the variables x and y of the solution for the second building block and interchanging the side lengths a and b in the same solution. We now have all of the building blocks.

Consider now the problem of analyzing stresses in the membrane depicted in Fig. 4. Two concentrated forces act on each of two opposite edges at distance δ from the corners. Other than this, the edges are completely traction free. We wish to analyze the stresses induced in the membrane by the concentrated forces. We accomplish this by means of a superposition of the three stress function building blocks described earlier.

We begin with the first building block. The concentrated forces of Fig. 4 are considered to act on this building block. By utilizing the Dirac function to represent these forces, we can easily represent them, in turn, by the series in Eq. (3). Therefore, the stress function for this building block is available. On top of this function we superimpose the second and third building block functions. Let us say we utilize k terms in the expansion of each of these latter two building blocks. Thus, there will be $2k$ unknown constants to be determined.

To evaluate these constants we proceed as follows. We expand the net shear stresses acting along the edges $y = b/2$ and $x = a$ of Fig. 4 in a suitable Fourier series. A cosine series is utilized here. We require that each coefficient in these two series should equal zero. It is noted that the first building block contributes to shear stress along the edge $x = a$ (Fig. 4) only. The foregoing procedure allows us to write $2k$ nonhomogeneous algebraic equations relating the $2k$ unknowns. This procedure is identical to that employed in Ref. 5 except that in the earlier work the equations are homogeneous.

We now solve the $2k$ simultaneous equations for the unknowns of the second and third building blocks. The stress distributions for the problem of Fig. 4 are immediately available, with the boundary conditions satisfied to any desired degree of accuracy by simply increasing the value of k to an appropriate level. Convergence is rapid.

Finally, let us focus on the problem of interest in this paper, as depicted in Fig. 5. This problem is easily decomposed into two problems by breaking the concentrated loads into their components, as represented by the broken lines in the figure. We first solve the problem obtained by deleting the horizontal components of the forces. Then we rotate the reference axis by 90 deg and solve the problem where only the horizontal force components of the figure are included. Finally, we properly superimpose the two sets of computed stresses to obtain the final stress distribution.

Two points of clarification should be made. Firstly, it is characteristic of the method of superposition as employed here that a small residue of shear force in the form of a high frequency wave of small uniform amplitude will remain along the edges. This resi-

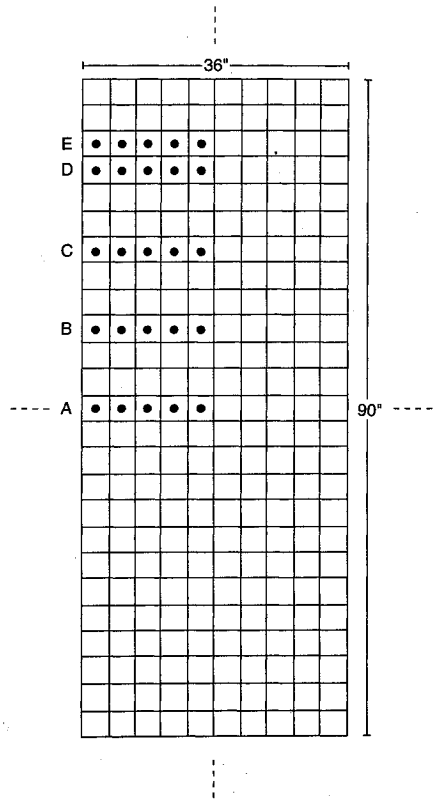

Fig. 7 Schematic representation of array of elements utilized in FE study: stress results reported here pertain to solid dot locations at levels A, B, etc.

due is of no consequence as adjacent small waves have the effect of cancelling out each other's effect along the edge. These residual stresses may cause small oscillations from the true stress, along the edges only. These oscillations can be made arbitrarily small by increasing the number of terms in the series. Secondly, since an infinite number of terms cannot be utilized, the integrals of the Dirac functions will not necessarily have unit area; and, furthermore, the forces will not be truly concentrated at a point. Practically, this causes no problem. A typical series representation of the Dirac function utilizing 10 terms is shown in Fig. 6. It will be noted that an applied force represented by this function is essentially concentrated at a dimensionless distance, $\delta/a = 0.05$, as required in this plot. Furthermore, using simple finite series integration, the exact area under the curve of Fig. 6 is easily obtained. This integral allows us to obtain the exact force being exerted on the membrane with the value of k selected.

Finite Element Approach

The finite element study was carried out utilizing version 67 of the finite element software, NASTRAN. A grid of four node quadrilateral plate elements was used to model the membrane. In such elements, the in-plane axial displacements are interpolated using bilinear basis functions. The stiffness matrices for each element are calculated based on the displacement method, or by the strain energy of the element as calculated through the basis functions, and assembled globally, node by node. The loads are set and the system is solved using one of the available solution sequences.

There are several solution sequences available in NASTRAN for solving the stresses in a structure. With a high degree of accuracy, the stresses can be solved using a solution sequence called SOL 64, which takes into account geometric nonlinearity. It does this by solving for the nodal displacements, altering the geometry of the model based on the current solution, and solving again. The user can specify the number of iterations. It was found for the membrane problem that there was at most a 0.013% error between the third and fourth iterations. From this solution, the displacements, the stresses in the x and y directions, shear stress, and the principal stresses and angles are available in numerical form. It may be noted that if SOL 64 detects buckling, it will neither finish its run nor provide a solution. In the region of corner loads buckling does occur, caused by slightly negative stress in one of the principal directions. To avoid this problem the out-of-plane degrees of freedom are eliminated from all of the grid points. This allows zones of compression to appear which are not strictly indicative of the true structural behavior of membranes, but these zones are localized to very small regions; however, it also allows the solution sequence to continue.

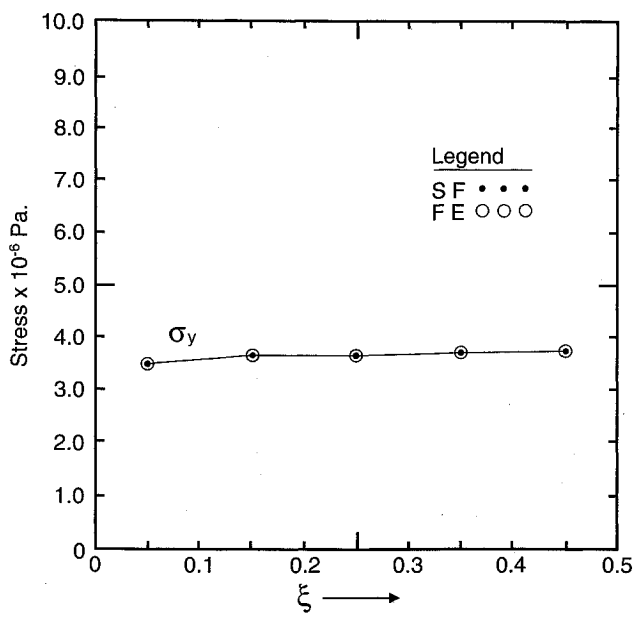

Fig. 8 Stresses at level A.

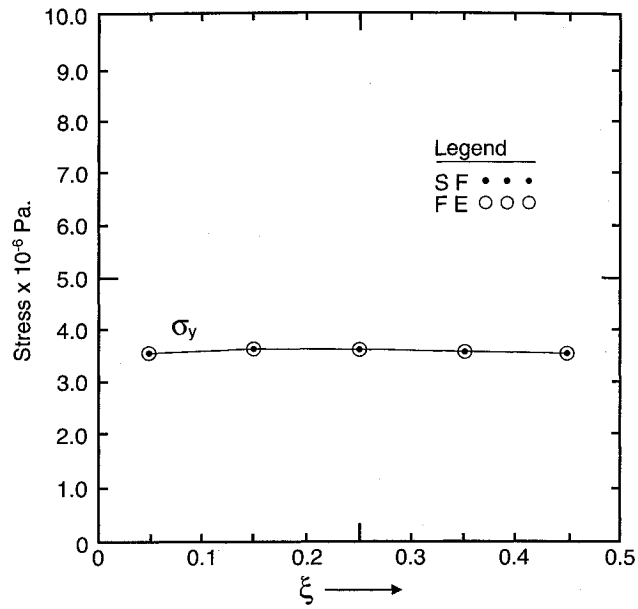

Fig. 9 Stresses at level B.

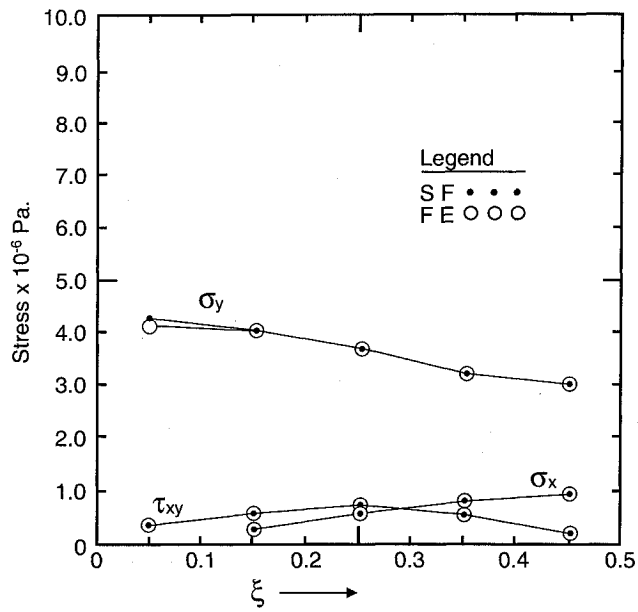

Fig. 10 Stresses at level C.

Presentation and Comparison of Computed Results

In accordance with the techniques described, stress analyses of two different rectangular membranes were conducted. One is a square membrane, 36 in. (91.44 cm) along each edge, with a thickness of 0.005 in. (0.127 mm) and a corner loading of 50 lb (222.41 N). The second membrane also has a width of 36 in. (91.44 cm) but with an aspect ratio of 2.5. It has the same corner loading of 50 lb (222.41 N) and thickness of 0.005 in. (0.127 mm). Very good agreement is found between the computed results of each method for each membrane. For this reason results are presented and compared for the nonsquare membrane only. It is also the more interesting problem since symmetry about the diagonals does not exist as is the case with the square membrane.

The finite element analysis for the nonsquare membrane was conducted utilizing the element scheme shown in Fig. 7. Stresses

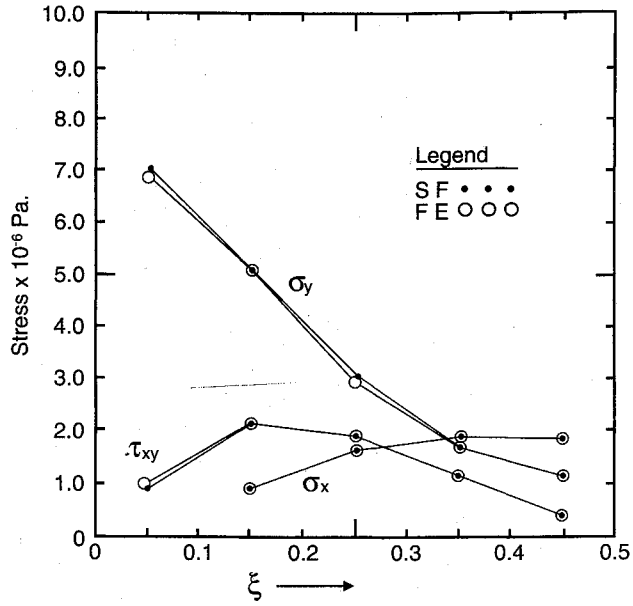

Fig. 11 Stresses at level D.

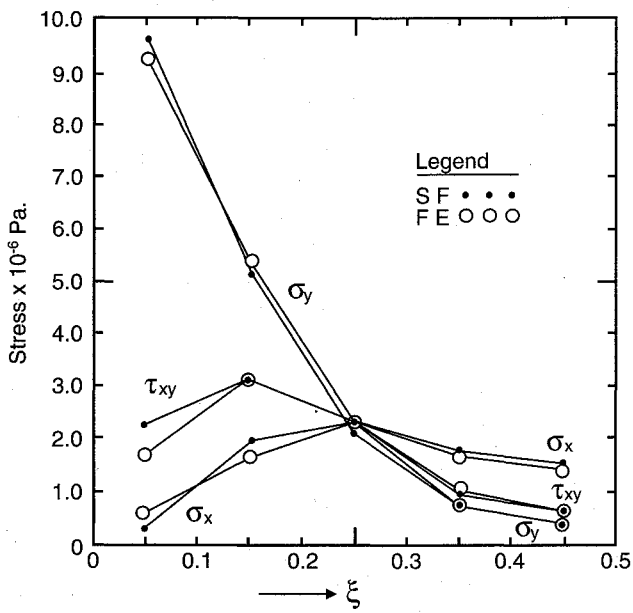

Fig. 12 Stresses at level E.

were computed and tabulated for the midpoints of these elements. It will be noted that 25 elements run in the long edge direction with 10 running in the direction of the short edge. Because of symmetry, the results relate to only a quarter of the elements of Fig. 7, say, the upper left quarter. Furthermore, small local differences in the two computed sets of results may occur in the corner region, depending on how the local loading is applied. In the case of the analytical-type studies, force distributions utilized are as depicted in Fig. 6, and the dimensionless loading distances from the corners (Fig. 5) are $\delta/a = \delta/b = 0.05$.

All of the results obtained through the analytical studies were computed using 10 terms in the series expansions of the Airy stress function. As is seen (Fig. 7), 250 elements were used in the finite element analysis. The coefficient matrix for the system of equations in the Airy stress function study, therefore, was 20 × 20. This is a very small matrix and larger matrices could easily have been handled. It was found, however, that in these stress computations convergence was very rapid. Utilizing more terms in the series would have introduced no change in the plotted results to be discussed shortly. In fact, this same rapid convergence is experienced when the superposition method is utilized to analyze plate vibration problems.

A word about membrane wrinkling is in order at this time. Wrinkling is a phenomenon that will occur at any point in a flexible membrane where one, or both, of the computed in-plane principal stresses becomes negative. Prediction of wrinkling is easily achieved with the analytical approach. One simply computes the in-plane normal and shear stresses for an entire grid of points throughout the membrane. From this set of stresses the two in-plane principal stresses are immediately computed and examined for the same grid of points. One of two possible outcomes will occur as follows.

1) All principal stresses are positive. This implies that no wrinkling occurs throughout the membrane and the solution for the stress distribution is valid. It is assumed here that the grid of points examined is of a sufficient density and of a sufficient area coverage so that results are representative of the entire membrane.

2) One or more principal stresses are negative at certain points in the grid. This implies that the stresses as computed are not totally correct. Wrinkling will initiate at points of indicated negative principal stress and resultant displacements and strains may affect the stresses at other points in the grid.

In the analytical-type studies reported here, no negative principal stresses were encountered. With the finite element approach certain small negative principal stresses were detected in the loaded corners of the membrane. This may be due to slight difference in the local application of statically equivalent corner loads. It was logically concluded that these low level negative stresses could effect stress and strain distributions in the immediate region of the applied load only, and for this reason their effects were suppressed as discussed earlier.

For purposes of presentation stresses at levels A–E only, as denoted in Fig. 7, are plotted. Each plot begins at the center of the element on the left-hand side of the figure and discrete values of the stresses are plotted for the central points of the first five elements moving to the right. In the plots, points are joined by simple straight lines.

The results of the study related to the nonsquare membrane are presented in Figs. 8–12. The legend in each figure denotes symbols utilized for representing stress function (SF) results and finite element (FE) results. It will be noted that the stresses σ_x and/or τ_{xy} are missing from some of the figures. This is because in such cases their values are close to zero.

It is seen that at level A, Fig. 8, the computed stresses from SF and FE predictions are so close that they are essentially coincident. This is the case in most plots. The stress σ_y is nearly uniform in this figure, and it is easily shown that its integral across the figure is almost exactly that required to balance the applied end loads. Because of symmetry, the computed shear stress at level A is 0.

Little difference is encountered in examining the stresses of level B, Fig. 9. This location is far enough from the membrane's short edges for this to be the case.

At level C, Fig. 10, good agreement continues between the computed stresses but now the stresses σ_x and τ_{xy} are no longer negligible. This, of course, is to be expected on moving out toward the membrane short edge and the point of loading.

At level D, Fig. 11, the stress σ_y is seen to be highly nonuniform. Toward the left of the figure the stress is of much greater magnitude as this represents the region immediately under and close to the loading point. The region to the right of the figure is not sufficiently removed from the loading point for the stresses to have diffused into this area.

At level E, Fig. 12, it is noted that the stress σ_y takes on very high values in the region under the loading point. It falls off rapidly to near-zero values on approaching the membrane long centerline. In this latter figure, small differences in the stress values computed by the two methods may be observed, mainly in the region under the load point. As mentioned earlier, such small differences are to be anticipated in this region due to the different ways in which the reactions of the applied concentrated forces on the membrane are modeled (see Fig. 4, for example). In general, we do not

require highly accurate solutions for the stresses at the immediate point of loading. As long as the applied load modeling gives us reactions on the membrane which are statically equivalent to the actual applied loads, our solutions for stresses will be very good in regions removed from the local loading area. It is seen here that there is also very good agreement between stress distributions obtained by each of the two methods of analysis.

Discussion and Conclusions

Stress distributions in corner loaded membranes have been computed by analytical means employing stress functions and also by means of a commercially available finite element method. Very good agreement is obtained when the two sets of computed results are compared. This attests to the mathematical validity of each method and indicates that they can be employed with confidence in future research and development work of this type.

Acknowledgment

The authors wish to acknowledge R. Hafer, SBR Project Manager, of the Department of National Defence, for supporting and funding this research activity.

References

[1]Tsandoulas, G. N., "Space-Based Radar," *Science*, Vol. 237, July 1987, pp. 257–262.

[2]Gorman, D. J., and Singal, R. K., "A Superposition-Rayleigh Ritz Method for Free Vibration Analysis of Non-Uniformly Tensioned Membranes," *Journal of Sound and Vibration*, Vol. 162, No. 3, 1993, pp. 489–502.

[3]Timoshenko, S. P., and Goodier, J. N., *Theory of Elasticity*, 3rd ed., McGraw-Hill, New York, 1987, pp. 46–52.

[4]Timoshenko, S. P., and Woinowsky-Krieger, S., *Theory of Plates and Shells*, 2nd ed., McGraw-Hill, New York, 1959, pp. 113, 114.

[5]Gorman, D. J., *Free Vibration Analysis of Rectangular Plates*, Elsevier North-Holland Co., 1981.